

Micellar stabilized single-walled carbon nanotubes for a pH-sensitive delivery of doxorubicin

F. Farvadi¹, A.M. Tamaddon^{2*}, S.S. Abolmaali², Z. Sobhani³ and G.H. Yousefi³

¹Student Research Committee, Shiraz University of Medical Science, School of Pharmacy, Shiraz, I.R. Iran.

²Center for Pharmaceutical Nanotechnology and Biomaterials, Pharmaceutical Sciences Research Center, School of Pharmacy, Shiraz University of Medical Science, Shiraz, I.R. Iran.

³Department of Pharmaceutical Sciences, School of Pharmacy, Shiraz University of Medical Science, Shiraz, I.R. Iran.

Abstract

Single-walled carbon nanotubes (SWNTs) are among the promising nano-devices for delivery of therapeutic agents. Yet the drastic hydrophobic natures of SWNTs make their handling and hence application difficult. Several researches have been conducted to make them more hydrophilic and water dispersible and less toxic. Among the different approaches, dispersion methods exploit different reagents such as surfactants and block copolymers. The question is whether these so called dispersed SWNTs are stable enough and suitable for biomedical applications. Herein we aimed to functionalize SWNT surface by dioleoylphosphatidylethanolamine-polyethylene glycol (PL-PEG) and sodium deoxycholate (SDC) micelles and compare their efficacy in SWNT stabilization for biomedical application such as delivery of doxorubicin. Shortening and water dispersion of SWNTs were carried out by ultrasonication in aqueous solutions at different concentrations of SDC or PL-PEG micelle and assessed by UV-Vis-NIR spectroscopy. The stability of SWNT dispersions were assessed over the time and in the presence of salt by macroscopic observation and UV-Vis-NIR spectroscopy. Doxorubicin loading and release were carried out under different pH conditions. SWNT dispersions were stable in water for at least several weeks at room temperature, but SDC prepared dispersions were prone to agglomeration in the presence of salt and doxorubicin. The critical PL-PEG concentration for stability in physiologic conditions was about 5 times its critical micelle concentration. Doxorubicin loading was pH dependent and its release was triggered in acidic condition of tumor medium.

Keywords: Single-walled carbon nanotube; Phospholipid-polyethylene glycol; Polymeric micelle; Doxorubicin

INTRODUCTION

Although most of the existing anticancer drugs are very potent, their efficacy is limited by their poor pharmacokinetic, systemic toxicity, and development of drug resistance. Many of these challenges may be overcome by development of efficient drug delivery systems. Among the numerous delivery systems currently under investigations, carbon nanotubes (CNTs) have shown great promise as novel delivery systems especially based on their ability to cross biological barriers (1). Pristine carbon nanotubes are made up of carbon atoms arranged in a series of condensed benzene rings and wrapped into a tubular form (2).

Single-walled carbon nanotubes (SWNTs), a kind of these novel polyaromatic molecules, have attracted considerable interest, as they offer potential advantages including ultra-high surface areas (that give them the ability to carry a high cargo loading of multiple molecules along the length of the nanotube sidewall) (3), high mechanical strength but ultra-light weight and structural flexibility (which could prolong the circulation time), ability to cross the biological barriers (which increase the bioavailability of the carried drug molecules and tumor accumulation), and excellent chemical and thermal stability (4-5). In cancer patients, SWNTs could have potential roles in delivering chemotherapeutics,

*Corresponding author: A.M. Tamaddon
Tel. 0098 711 2424127, Fax. 0098 711 2424126
Email: amtamadon@gmail.com

diagnostic imaging agents, DNA, small interfering RNA, and proteins to detect or treat cancer cells (5).

SWNTs have highly hydrophobic surfaces, and their dispersions are not stable in aqueous phase. For biomedical applications, surface chemistry or functionalization is required to solubilize CNTs, and to render biocompatibility and low toxicity. Various reagents including surfactants (6-9), peptides (10-12), DNA (13) and polymers (14-15), have been exploited to disperse SWNTs in water. Sodium deoxycholate salts (16-17), Sodium dodecyl sulfate and Tween 20 (7) and hexahydroxytriphenylene hydrate (18) are examples of the used surfactants. On the other hand it has been reported that modifying SWNTs by attaching hydrophilic polymers such as poly ethylene glycol (PEG) yield SWNT-polymer conjugates stable in biological environments (19-20). Apart from solubilization of CNTs, PEGylation is one of the most effective methods to prolong the blood-circulation time due to the known “stealth” properties of polyethylene glycol (PEG) to overcome the phagocytic activity of the reticulo-endothelial system (13), keeping the nanotubes circulating in the bloodstream long enough (much longer than free medication) to find their way to the target location resulting in significantly increased therapeutic efficacy (21). Moreover PEGylation provide a platform for further modifications such as conjugating specific ligands toward biologic targets.

Doxorubicin (DOX) is an anthracycline antineoplastic antibiotic which may act by forming a stable complex with DNA and interfering with the synthesis of nucleic acids (22). While DOX has been extensively used in the clinic to treat ovarian, breast, lung, uterine and cervical cancers, its efficiency is limited due to cardiotoxicity and development of drug resistance. So application of efficient and targeted delivery of DOX to neoplastic lesions would lower non-specific toxicity and increases the clinical utility of DOX (23). Because of their polyaromatic surface, SWNTs are suitable for the delivery of aromatic drugs such as DOX, which are directly loaded on the nanotube surface via π - π stacking (3,19).

Polymeric micelles have recently attracted much attention as self-assembled delivery

systems or further surface modification of hydrophobic substrates. These micelles have unique characteristics such as uniform nanosize, core-shell architecture, and a good thermodynamic stability in physiological conditions because of their low critical micelle concentration (CMC) (24). PEG shell imparts “stealth” properties of the micelle without the need of chemical conjugation.

Herein we aimed to develop and characterize physico-chemically SWNT dispersion stabilized by either dioleoylphosphatidylethanolamine-polyethylene glycol (PL-PEG) polymeric micelles or sodium deoxycholate (SDC) micelles and their potential application for a sustained and pH-sensitive delivery of DOX.

MATERIALS AND METHODS

Materials

Our starting materials were powder of high-pressure carbon monoxide decomposition (Hipco) SWNTs (purity, >90%, mean diameter ~ 1-2 nm, length ~ 1-3 μ m, SSA 380 m²/g) Neutrino Co., Germany, dioleoylphosphatidylethanolamine-polyethylene glycol (PL-PEG) JenKem, USA, sodium deoxycholate (SDC) Sigma Aldrich, USA, and Doxorubicin hydrochloride (Adriblastina[®]) Pharmacia, Italy.

Preparation and characterization of PL-PEG micelles

For the preparation of PL-PEG polymeric micelles, the polymer was dissolved in chloroform, and then the chloroform was evaporated from polymer by vacuum rotary evaporation at 30°C for 4 h. The dried film was rehydrated by adding 20 mM 4-(2-hydroxyethyl)-1-piperazineethanesulfonic acid (HEPES) buffer solution pH 7.4 and 5 min vortex (25,26). The SDC micelles were prepared by simply dissolving the dry powder in deionized water.

The critical micelle concentration (CMC) of PL-PEG was determined by pyrene fluorescence method (26); from a stock solution of 1 mg.ml⁻¹ pyrene dissolved in chloroform, 10 μ l aliquots was transferred into a series of clean, dry microtubes and the solvent allowed to evaporate under vacuum by protecting from light to get 10 μ g of dry pyrene. A series of polymer solutions (0.1-100

μM) in 20 mM HEPES buffer solution were added to dry pyrene. Pyrene concentration in each tube was 50 μM . The mixtures were shaken in dark for 20 h at 25°C. The fluorescence intensity of solubilized pyrene in micellar phase was determined spectrofluorometrically at wavelengths of excitation (λ_{ex}) 320 nm and emission (λ_{em}) 380 nm.

Optimizing SWNT dispersion by micellar ultrasonication

SWNT was ultrasonicated by probe-sonicator (Hielscher UP200H, 200 W and 50% amplitude) in 100 μM PL-PEG or 10 mM SDC micelle solution (CMC=2 mM, provided by the manufacturer) for different hours (up to 12 h) to disrupt SWNT bundles and simultaneously stabilize the isolated SWNTs through surface adsorption of PL-PEG molecules. The sample tube was surrounded by an ice-jacket to keep the temperature low. The ultrasonic wave was exploited in a pulse mode (0.5 cycle per second) to allow micelle monomers settling down to SWNT surface. At given time intervals sampling was done and particle size analysis and UV-Vis-NIR spectroscopy carried out at $\lambda=808$ nm (19,27) to estimate the fraction of solubilized SWNT in aqueous phase against ultrasonication time. Particle size was analyzed as a means to study the effect of ultrasonication time on exfoliation of SWNT bundles; 1 ml of each sample was 10 times diluted to give 10 ml of 20 $\mu\text{g}\cdot\text{ml}^{-1}$ SWNT for particle size analysis by laser light scattering method (SALD-2101, Simadzu, Japan).

Repeated cycles of ultracentrifugation (140,000 g for 1 h) and washing were carried out to remove excess of unbound reagents remaining in the supernatant if intended.

To remove the non-dissociated SWNTs remain as small bundles even after complete dispersion, centrifugation was carried out. Optimum centrifugation condition was determined after trying several sets of speed and duration by optical microscopic inspection after each centrifugation run.

To optimize dispersion efficiency, SWNTs were ultrasonicated at different concentrations of SDC or PL-PEG solution for appropriate time. The maximum absorbance of 1.2 was determined by UV-Vis-NIR spectropho-

meter at 808 nm for accurately weighed 1 mg SWNT that was fully dispersed in 5 ml total volume. Dispersion efficiency was calculated as follows,

$$\text{Dispersion Efficiency} = \frac{\text{NIR absorbance at } \lambda 808 \text{ nm} \times 100}{\text{Maximum absorbance at } \lambda 808 \text{ nm}}$$

To measure SWNT concentration, a stock of SWNT dispersion of known concentration was prepared in either of SDC or PL-PEG micelle solutions by ultrasonication. UV-Vis-NIR spectroscopy was performed for various concentrations of SWNT prepared by serial dilution of stock solution. Absorbance at $\lambda=808$ nm versus SWNT concentration was plotted for measuring SWNT concentration (mass extinction coefficient: $3.74 \times 10^{-2} \text{ g}\cdot\text{L}^{-1}\cdot\text{cm}^{-1}$, $R^2=0.9999$).

Stability of SWNT dispersions

To compare the effectiveness of micellar dispersions of SWNT, their stability were assessed according to incubation time, exposure to salt (isotonic NaCl; 0.9%) and upon dilution of micellar dispersion either by visual inspection of agglomerate formation or sedimentation, or UV-Vis-NIR spectroscopy at $\lambda=808$ nm as previously described.

DOX loading onto the dispersed nanotubes

Various concentrations of DOX hydrochloride (0.1 to 1 mg/ml) was simply mixed with the dispersed SWNTs at a nanotube concentration of $\sim 50 \mu\text{g}/\text{ml}$ in phosphate buffer solutions at different pH values (8.5, 7.4, 5.5) at 4°C overnight. Just prior to removal of free DOX, fluorescence spectra of the samples were depicted by fluorimetry ($\lambda_{\text{ex}}=495$) in comparison with DOX solution to characterize DOX loading on stabilized SWNT.

Unbound free DOX was removed by centrifugation and washed thoroughly by repeated ultrafiltration through a 100 KDa Amicon® ultrafiltration filter with deionized water until the filtrate became reddish color free (corresponding to about 5 times washing). The formed complexes (referred to as DOX-SWNT) were then resuspended and stored at 4°C. The amount of DOX loaded onto SWNTs was measured by the absorbance peak of the supernatant (free DOX) at 490 nm according

to the calibration curve. The loading efficiency and the loading capacity of SWNT for different DOX/SWNT ratios were calculated according to the below equations:

$$\% \text{ Loading Efficiency} = \left(1 - \frac{\text{DOX Conc. of Supernatant}}{\text{Initial Conc. of DOX}}\right) \times 100$$

$$\% \text{ Loading Capacity} = \frac{\% \text{ Loading Efficiency} \times \text{Initial Conc. of DOX}}{\text{SWNT Conc.}}$$

Loading factor was defined to compare loading processes performed at different pH values.

$$\text{Loading Factor} = \frac{\text{Loading efficiency} \times 100}{\text{Maximum loading efficiency}}$$

DOX release from the nanotubes

The DOX-SWNT complexes were allowed to stand at 37°C in saline supplemented 20 mM phosphate buffer solution (pH 7.4 and pH 5.5) while shaking at 300 rpm. After different time intervals, the SWNTs were separated from the buffer by centrifugation, and the concentration of released DOX in the supernatant was estimated by UV-Vis spectroscopy at $\lambda=490$ nm as described previously. The experiment was run in triplicate.

RESULTS

Determination of critical micelle concentration of PL-PEG micelles

Fluorescence intensity of 50 μM pyrene solution at $\lambda_{\text{ex}}=320$ nm and $\lambda_{\text{em}}=380$ nm was

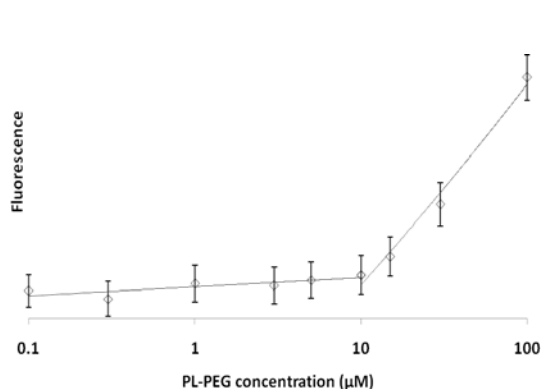


Fig. 1. Fluorescence intensity of 50 μM pyrene in different concentrations of PL-PEG.

plotted against increasing concentrations of PL-PEG in a semi-logarithmic scale (Fig. 1). Wherever PL-PEG concentration passed through unknown critical micelle concentration (CMC), it increased pyrene solubility and hence the slope of pyrene fluorescence intensity changed very significantly. The CMC was determined to be about 10 μM .

Optimizing SWNT dispersion by micellar ultrasonication

The optimum ultrasonication duration was determined to be about 8 h by UV-Vis-NIR spectroscopy at 808 nm (Fig. 2). According to the particle size analysis results, increasing ultrasonication time could decrease SWNT bundles as well as bundle size. Fig. 3 shows that the bimodal size distribution converted to a unimodal distribution by eliminating the large particles in micron range. This leads to a decrease in the range of size distribution (Table 1).

SWNT dispersion efficiency was dependent on the type and concentration of the micelle constituting monomers. Study of different concentrations of SDC and PL-PEG showed that the effective concentration for most dispersion of SWNTs is 10 and 0.1 mM respectively (Fig. 4); about 2-5 times of CMC for SDC and about 10 times for PL-PEG. The effective concentration observed for SDC was in agreement with the findings of Park and Seong who have reported the optimum concentration of SDC for SWNT dispersion 12 mM (0.5 w%) (16).

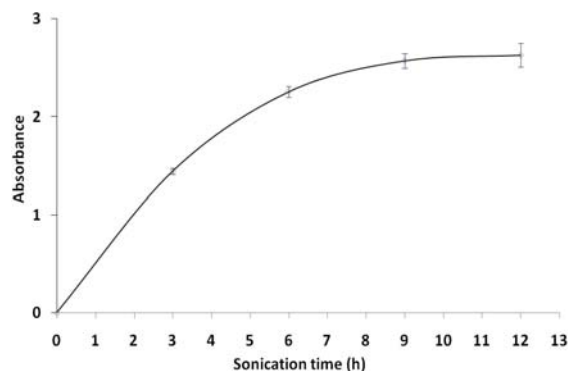


Fig. 2. Effect of ultrasonication (24 KHz, 200 watt, 50% intensity, 0.5 cycle/sec) on SWNT dispersion as determined by UV-Vis-NIR absorbance at 808 nm (error bars represent mean \pm SD, n=3).

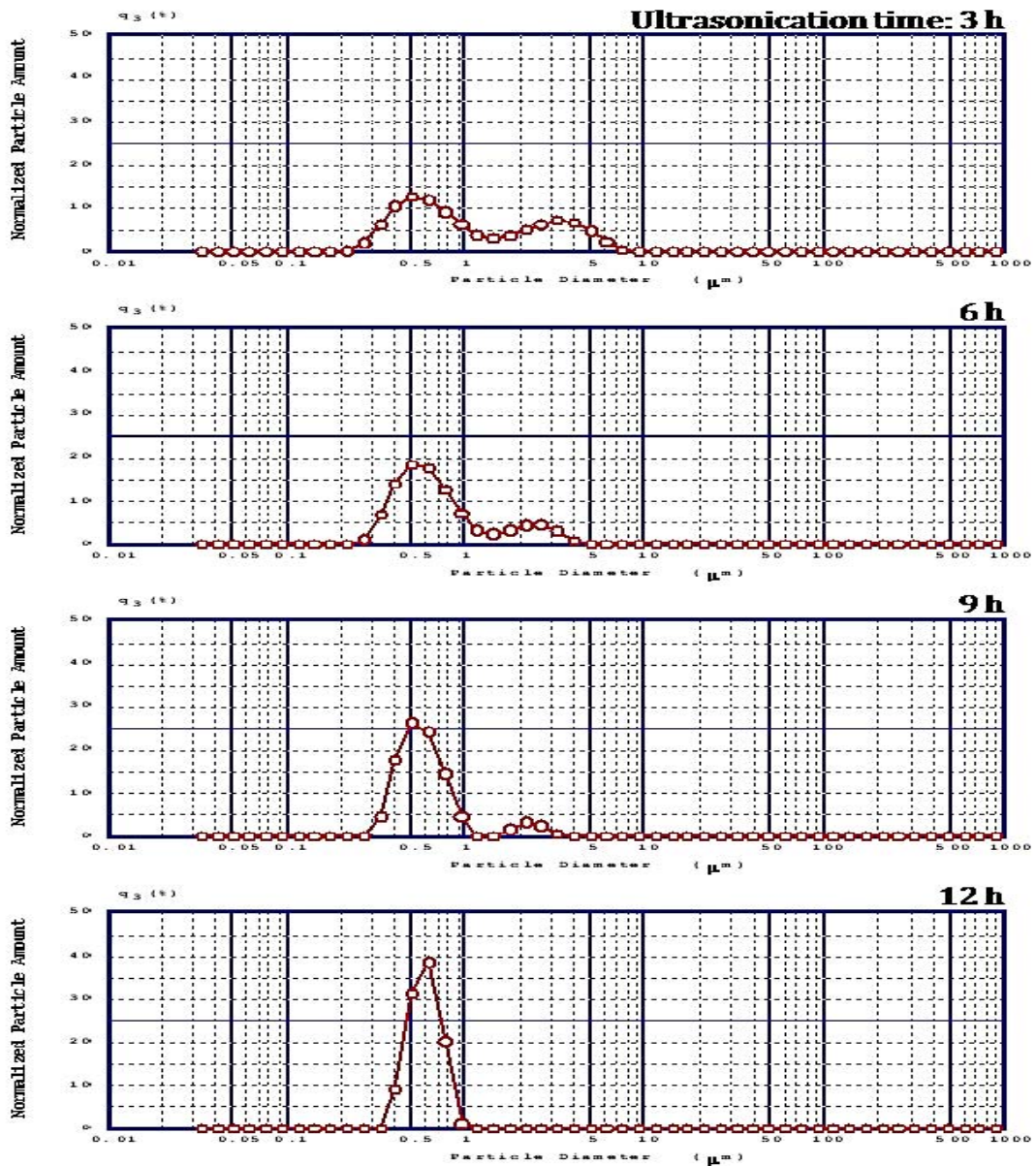


Fig. 3. Volume size distribution graphs of 20 μm SWNT in 100 μM PL-PEG.

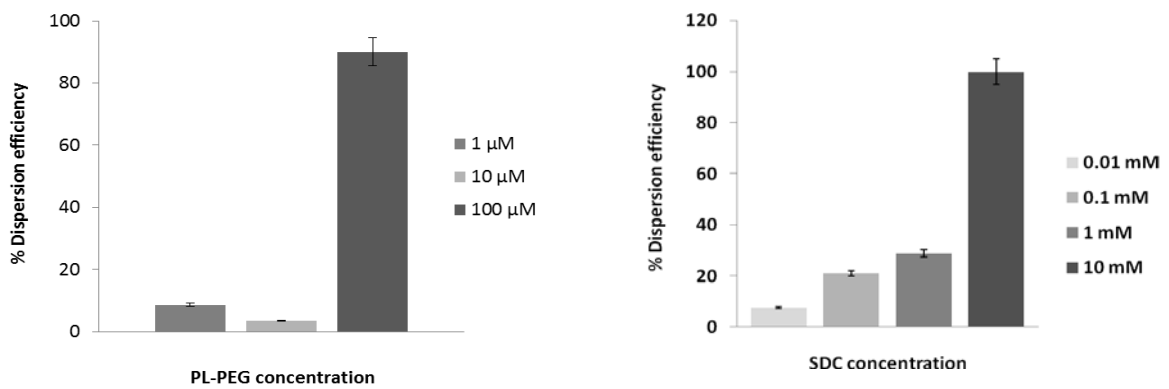


Fig. 4. Dispersion efficacy of SWNT at different concentrations of PL-PEG (A) and sodium deoxycholate (SDC) (B)

Table 1. Size distribution parameters for 20 μ M SWNT in 100 μ M PL-PEG

	Ultrasonication time (h)	Size distribution range [μ m]	Modal diameters [μ m]		Mean diameter [μ m]
Volume distribution	3	0.196-6.746	0.562	3.611	1.064 \pm 0.393
	6	0.241-0.611	0.562	2.932	0.734 \pm 0.277
	9	0.241-2.932	0.562	2.381	0.617 \pm 0.210
	12	0.365-0.840	0.562	-	0.583 \pm 0.082
Number distribution	3	0.196-5.477	0.355		0.391 \pm 0.142
	6	0.196-3.611	0.355		0.420 \pm 0.420
	9	0.241-2.932	0.447		0.442 \pm 0.110
	12	0.365-0.682	0.562		0.527 \pm 0.077

Table 2. Comparison of sodium deoxycholate (SDC) and PL-PEG stabilized SWNT regarding their dispersion efficiency and salt stability at different concentrations

Dispersing agent	Concentration (μ M)	Ratio to SWNT (w/w)	Dispersion efficiency %	Salt stability
SDC	10	0.008	7.76	✗
	100	0.8	21.12	✗
	1,000	8	28.88	✗
	10,000	80	100	✗
PL-PEG	1	0.015	8.62	✗
	10	0.15	3.45	✗
	100	1.5	90.09	✓

✗: SWNT sedimentation against salt addition; ✓: SWNT stability against salt addition

Centrifugation was performed to obtain uniform dispersion of isolated SWNTs. However, as it is already shown, not only the residual bundled SWNTs, but also some parts of the single ones are removed during the process (16). Therefore the optimum centrifugation speed and time for maximum removal of SWNT bundles and minimum reduction in SWNT concentration was determined to be 2000 g for 15 min. SWNT recovery was about 64-67% as determined by UV-Vis-NIR spectroscopy at $\lambda=808$ nm.

Stability of SWNT dispersions

The dispersions of SWNTs were stable in water for at least several weeks at room temperature without aggregating and precipitating out of the solution and were uniform macro and microscopically.

Although PL-PEG-SWNTs were acceptably stable over time and against salt exposure, after complete removal of free PL-PEG they were prone to agglomeration in the presence of salt (especially in alkaline pH (≥ 8.5)). The critical PL-PEG concentration required for a stable SWNT dispersion was about 5 times its CMC (C \sim 50-100 μ M) (Table 2). Moreover, if excess unbound PL-PEG was removed before loading step, SWNTs would agglomerate in presence of DOX or in alkaline medium

required for the loading process. Similarly any dilution below PL-PEG critical concentration could destabilize PL-PEG-SWNT dispersions.

PL-PEG modified SWNTs maintained their dispersion much better in high pHs (pH \sim 8-8.5) than in acidic pH, in other words they readily regained their dispersion after centrifugation induced sedimentation in alkaline conditions while formed tough sediments in low pH (\sim 5.5).

In comparison with PL-PEG, SDC treated SWNT dispersion was much less stable in the presence of salt and similarly under physiologic conditions and it tends to agglomerate immediately since salt ions could detach SDC molecules from SWNT surface readily. Therefore such nanotubes were not capable to stand loading with DOX. Table 2 summarizes the comparison of SDC and PL-PEG.

DOX loading onto the nanotubes

After overnight incubation of the dispersed SWNT with DOX at different acidic conditions, complex formation was proved by fluorescence quenching of loaded DOX compared with free DOX solution at the same concentration (19) (Fig. 5).

Free unbound DOX was thoroughly removed by repeated washing to retain only the DOX-SWNT complexes. Formation of

DOX-SWNT complex was also evidenced by the reddish color of DOX-SWNT samples after free DOX removal, due to adsorbed DOX and its characteristic UV-Vis absorbance peak at 490 nm on top of the characteristic SWNT absorption spectrum (Fig. 6).

The amount of doxorubicin bound onto SWNTs was pH-dependent, decreasing loading factor (defined as loading efficiency/maximum efficiency) from 100 to ~19.5 to ~11 as pH was reduced from 8.5 to 7.4 and 5.5 respectively (Fig. 7).

On the basis of optical absorbance data, we estimated loading efficiency to be ~30% and loading capacity to be ~410% in respect to nanotubes weight, which is very similar to Liu and coworkers' result who have reported 400% loading capacity for DOX loaded onto SWNT (19). The loading efficiency of DOX

increases as its concentration increases from 0.1 to 1 mg/ml corresponding to DOX:SWNT ratio of 2 to 20 W/W (Fig. 8).

The DOX-SWNT dispersions settled down after overnight incubation (at refrigerator or room temperature) but they did not aggregate nor form tough cakes but rather were readily re-dispersed by minimal force.

DOX release from the nanotubes

The release of the DOX loaded on SWNTs was pH-stimulated, triggered at acidic pH (Fig. 9). The release profile was much sustained at neutral pH with a burst release at early times. We found that DOX release also depends on the slight amounts of free DOX in equilibrium with loaded DOX. In other words, dilution can affect release via altering equilibrium between free and bounded DOX.

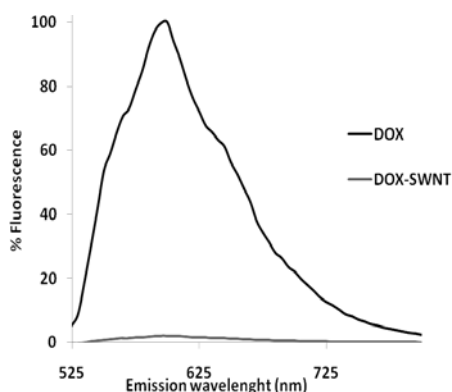


Fig. 5. Fluorescence quenching of doxorubicin after loading on 50µg.ml⁻¹ SWNT at pH 8. A significant fluorescence quenching was evident for doxorubicin bound to SWNT.

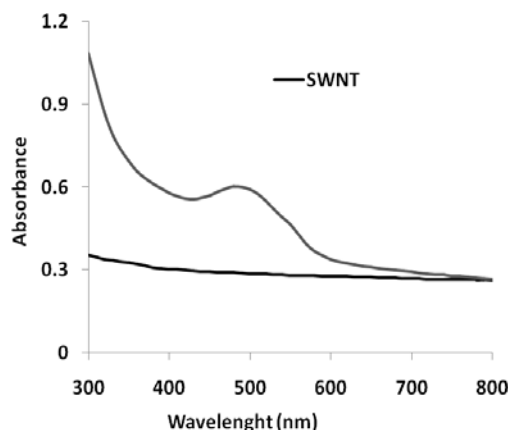


Fig. 6. UV-Vis-NIR absorbance spectrum of PL-PEG stabilized SWNT, doxorubicin loaded or alone.

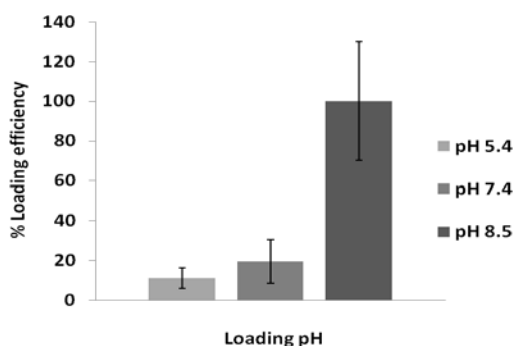


Fig. 7. Effect of pH on loading efficiency of doxorubicin on PL-PEG-SWNT (error bars represent mean \pm SD, n=3)

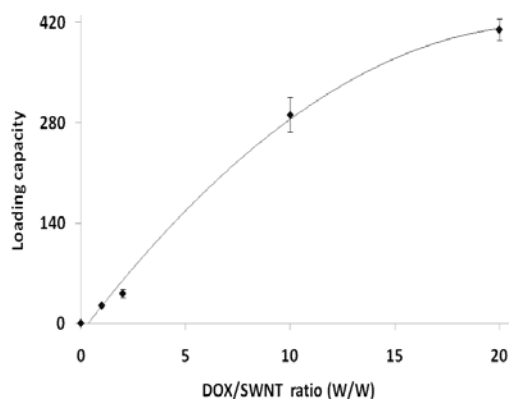


Fig. 8. Correlation between the loading capacity of PL-PEG-SWNT and doxorubicin concentration.

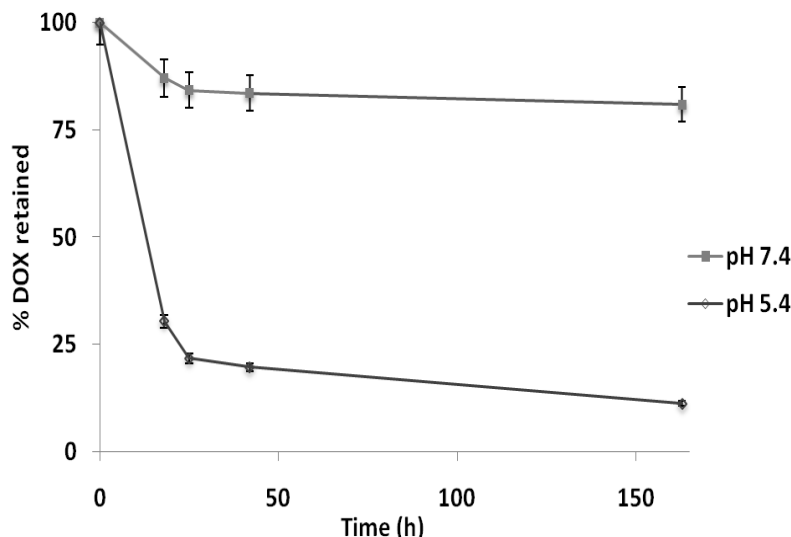


Fig. 9. The release profile of doxorubicin loaded on PL-PEG-SWNT in different media at 37°C.

DISCUSSION

Since the SWNTs are extremely hydrophobic, they have to be well dispersed and stabilized prior to biomedical applications. Similarly the stabilization method should be stable enough to bear physiologic conditions and prevent SWNT agglomeration *in vivo*.

While ultrasonication leads to exfoliation of SWNTs into isolated tubes, adsorption of the PL-PEG copolymers causes repulsion among the polymer-decorated SWNTs leading to stabilization of the SWNT dispersion forming a macroscopically homogeneous dispersion (Fig. 2). Some researchers (27-28) believe that UV-Vis-NIR absorbance qualitatively determines the nanotube dispersion state and evidence isolated SWNTs rather than large aggregates because only individual or small bundles of SWNT exhibit sharp absorbance peaks, while large bundles exhibit only monotonically decreasing absorbance with increasing wavelength. So according to UV-Vis-NIR spectroscopy (Fig. 2), dispersion quality was extensively dependent on the ultrasonication duration. Ultrasonication not only progress SWNT dispersion, but also simultaneously shortens the nanotube length, i.e., reduces the aspect ratio (28-29) to be applicable for biological applications. Moniruzzaman and coworker believe that the minimum sonication conditions (time and

power) that produce CNT degradation are certainly depend on nanotube concentration and initial nanotube length distribution (28).

Particle size analysis based on light scattering method was useful in detection of SWNT bundles (Fig. 3) but it doesn't seem to be suitable for reporting the mean size since isolated SWNTs have aspect ratios very far from one unit. Instead, microscopy techniques such as atomic forced microscopy could be used that is under investigation in our laboratory.

The colloidal stability of PL-PEG modified SWNTs was concentration-dependent. Although PL-PEG modified SWNTs showed more stability in comparison with SDC treated nanotubes, it does not seem to be an appropriate candidate for SWNT stabilization for biomedical applications since it might be prone to instability in harsh conditions and could not bear a complete micelle removal. This may probably happens because of the low stability constant of PL-PEG association on SWNT surface; however, regarding the very low CMC of PL-PEG, the later can be solved easily by increasing the micellar concentration as experienced by some research groups for delivery of different chemotherapeutic agents.

Considering the pH-dependency of DOX loading (Fig. 7), it seems to be due to deprotonation of amine group of DOX molecule in alkaline pH and hereupon settling onto the SWNT surface which poses

polyaromatic structure and hence can get involved in π - π stacking with DOX molecule. Again regarding acidic pH-stimulating behavior of the release profile, the mechanism is probably getting positive ion charge due to protonation of amine group of DOX molecule and therefore enhanced aqueous solubility and detachment from the carrier surface.

CONCLUSION

Since the SWNTs are extremely hydrophobic, it has to be well dispersed and stabilized prior to biomedical applications. Similarly the stabilization method should be stable enough to bear physiologic conditions and prevent SWNT agglomeration *in vivo*. Therefore based upon our finding, SDC reagent seems to be less efficient for biomedical applications than PL-PEG stabilization method. Taking into consideration the high level of DOX loading especially at alkaline pH and a triggered release at low acidic pH of tumor medium, these could make SWNTs potentially an efficient carrier for *in vivo* DOX delivery since the micro-environments in the extracellular tissues of tumors and intracellular lysosomes and endosomes are acidic. Moreover, a much sustained release of DOX in neutral pH guarantees preservation of the loaded amount while the nanotubes circulating in blood stream. Therefore, the carrier is proposed to be evaluated in cell culture and for pharmacokinetic and pharmacodynamic studies in animal model.

ACKNOWLEDGMENT

This work was financially supported by Shiraz University of Medical Sciences and carried out as a partial fulfillment of Ms. Farvadi thesis.

REFERENCES

1. Ali-Boucetta H, Al-Jamal KT, McCarthy D, Prato M, Bianco A, Kostarelos K. Multiwalled carbon nanotube-doxorubicin supramolecular complexes for cancer therapeutics. *Chem Commun.* 2008;4:459-461.
2. Pastorin G. Crucial functionalizations of carbon nanotubes for improved drug delivery: a valuable option? *Pharm Res.* 2009;26:746-769.
3. Liu Z, Tabakman S, Welsher K, Dai H. Carbon nanotubes in biology and medicine: In vitro and in

4. Lin Y, Taylor S, Li H, Fernando KAS, Qu L, Wang W, *et al.* Advances toward bioapplications of carbon nanotubes. *J Mater Chem.* 2004;14:527-541.
5. Gannon CJ, Cherukuri P, Yakobson BI, Cognet L, Kanzius JS, Kittrell C, *et al.* Carbon nanotube-enhanced thermal destruction of cancer cells in a noninvasive radiofrequency field. *Cancer.* 2007;110:2654-2665.
6. Haggemueller R, Rahatekar SS, Fagan JA, Chun J, Becker ML, Naik RR, *et al.* Comparison of the quality of aqueous dispersions of single wall carbon nanotubes using surfactants and biomolecules. *Langmuir.* 2008;24:5070-5078.
7. Datsyuk V, Landois P, Fitremann J, Peigney A, Galibert AM, Soula B, *et al.* Double-walled carbon nanotube dispersion via surfactant substitution. *J Mater Chem.* 2009;19:2729-2736.
8. Moore VC, Strano MS, Haroz EH, Hauge RH, Smalley RE, Schmidt J, *et al.* Individually suspended single-walled carbon nanotubes in various surfactants. *Nano Lett.* 2003;3:1379-1382.
9. Ishibashi A, Nakashima N. Strong chemical structure dependence for individual dissolution of single-walled carbon nanotubes in aqueous micelles of biosurfactants. *Bull Chem Soc Jpn.* 2006;79:357-359.
10. Dieckmann GR, Dalton AB, Johnson PA, Razal J, Chen J, Giordano GM, *et al.* Controlled assembly of carbon nanotubes by designed amphiphilic peptide helices. *J Am Chem Soc.* 2003;125:1770-1777.
11. Nicolosi V, Cathcart H, Dalton AR, Aherne D, Dieckmann GR, Coleman JN. Spontaneous exfoliation of single-walled carbon nanotubes dispersed using a designed amphiphilic peptide. *Biomacromolecules.* 2008;9:598-602.
12. Ortiz-Acevedo A, Xie H, Zorbas V, Sampson WM, Dalton AB, Baughman RH, *et al.* Diameter-selective solubilization of single-walled carbon nanotubes by reversible cyclic peptides. *J Am Chem Soc.* 2005;127:9512-9517.
13. Liang F, Chen B. A review on biomedical applications of single-walled carbon nanotubes. *Curr Med Chem.* 2010;17:10-24.
14. Ntim SA, Sae-Khow O, Witzmann FA, Mitra S. Effects of polymer wrapping and covalent functionalization on the stability of MWCNT in aqueous dispersions. *J Colloid Interface Sci.* 2011;355:383-388.
15. O'Connell MJ, Boul P, Ericson LM, Huffman C, Wang Y, Haroz E, *et al.* Reversible water-solubilization of single-walled carbon nanotubes by polymer wrapping. *Chem Phys Lett.* 2001;342:265-271.
16. Park J, Seong MJ. Dispersion efficiency of carbon nanotubes in aqueous solutions of deoxycholate sodium salts. *J Korean Phys Soc.* 2010;56:1391-1394.
17. Xu H, Abe H, Naito M, Fukumori Y, Ichikawa H, Endoh S, *et al.* Efficient dispersing and shortening of super-growth carbon nanotubes by ultrasonic treatment with ceramic balls and surfactants. *Adv Powder Technol.* 2010;21:551-555.

18. Yamamoto T, Motoyanagi J, Murakami Y, Miyauchi Y, Maruyama S, Kato M. Improved bath sonication method for dispersion of individual single-walled carbon nanotubes using new triphenylene-based surfactant. *Jpn J Appl Phys.* 2008;47:2000-2004.
19. Liu Z, Sun X, Nakayama-Ratchford N, Dai H. Supramolecular chemistry on water-soluble carbon nanotubes for drug loading and delivery. *ACS Nano.* 2010;4:7726.
20. Chattopadhyay J, de Jesus Cortez F, Chakraborty S, Slater NKH, Billups WE. Synthesis of water-soluble pegylated single-walled carbon nanotubes. *Chem Mater.* 2006;18:5864-5868.
21. Robertson FM, Ferrari M. Introduction and rationale for nanotechnology in cancer therapy. In: Amiji MM, editor. *Nanotechnology for cancer therapy.* Boca Raton: Talor & Francis Group; 2007. p. 3-10
22. Martindale W. *The complete drug reference.* 37th ed. Sweetman SC, editor. London: Pharmaceutical Press; 2011; p. 780.
23. Kohli A. Cell and nanomaterial-based approaches for diagnosis and chemotherapy of metastatic cancer cells. Massachusetts Institute of Technology; 2010. p. 40
24. Tian H, Deng C, Lin H, Sun J, Deng M, Chen X, *et al.* Biodegradable cationic PEG-PEI-PBLG hyperbranched block copolymer: synthesis and micelle characterization. *Biomaterials.* 2005;26:4209-4217.
25. Ashok B, Arleth L, Hjelm RP, Rubinstein I, Onyuksel H. In vitro characterization of PEGylated phospholipid micelles for improved drug solubilization: effects of PEG chain length and PC incorporation. *J Pharm Sci.* 2004;93:2476-2487.
26. Sezgin Z, Yuksel N, Baykara T. Preparation and characterization of polymeric micelles for solubilization of poorly soluble anticancer drugs. *Eur J Pharm Biopharm.* 2006;64:261-268.
27. Kam NWS, O'Connell M, Wisdom JA, Dai H. Carbon nanotubes as multifunctional biological transporters and near-infrared agents for selective cancer cell destruction. *Proceedings of the National Academy of Sciences of the United States of America.* 2005;102:11600-11605.
28. Moniruzzaman M, Winey KI. Polymer nanocomposites containing carbon nanotubes. *Macromolecules.* 2006;39:5194-5205.
29. Won KP, Jung HK, Lee SS, Kim J, Lee GW, Park M. Effect of carbon nanotube pre-treatment on dispersion and electrical properties of melt mixed multi-walled carbon nanotubes/poly (methyl methacrylate) composites. *Macromol Res.* 2005;13:206-211.